Polestar: An Intelligent, Efficient and National-Wide Public Transportation Routing Engine

Hao Liu[1], Ying Li[2], Yanjie Fu[3], Huaibo Mei[2], Jingbo Zhou[1], Xu Ma[2], Hui Xiong[4*]
[1]Business Intelligence Lab, Baidu Research, [2]Baidu Maps, Baidu Inc., [3]University of Central Florida, [4]Rutgers University
[1,2]{liuhao30, liying, meihuaibo, zhoujingbo, maxu}@baidu.com, [3]yanjie.fu@ucf.edu, [4]hxiong@rutgers.edu

ABSTRACT

Public transportation plays a critical role in people's daily life. It has been proven that public transportation is more environmentally sustainable, efficient, and economical than any other forms of travel [3, 15]. However, due to the increasing expansion of transportation networks and more complex travel situations, people are having difficulties in efficiently finding the most preferred route from one place to another through public transportation systems. To this end, in this paper, we present Polestar, a data-driven engine for intelligent and efficient public transportation routing. Specifically, we first propose a novel Public Transportation Graph (PTG) to model public transportation system in terms of various travel costs, such as time or distance. Then, we introduce a general route search algorithm coupled with an efficient station binding method for efficient route candidate generation. After that, we propose a two-pass route candidate ranking module to capture user preferences under dynamic travel situations. Finally, experiments on two real-world data sets demonstrate the advantages of Polestar in terms of both efficiency and effectiveness. Indeed, in early 2019, Polestar has been deployed on Baidu Maps, one of the world's largest map services. To date, Polestar is servicing over 330 cities, answers over a hundred millions of queries each day, and achieves substantial improvement of user click ratio.

KEYWORDS

Public transportation routing; context-aware ranking; route recommendation; deployment

ACM Reference Format:
Hao Liu, Ying Li, Yanjie Fu, Huaibo Mei, Jingbo Zhou, Xu Ma, Hui Xiong. 2020. Polestar: An Intelligent, Efficient and National-Wide Public Transportation Routing Engine. In *the 26th ACM SIGKDD Conference on Knowledge Discovery and Data Mining (KDD'20), August 23–27, 2020, Virtual Event, USA.* ACM, New York, NY, USA, 9 pages. https://doi.org/10.1145/3394486.3403281

*Corresponding author.

KDD '20, August 23–27, 2020, Virtual Event, CA, USA

ACM ISBN 978-1-4503-7998-4/20/08…$15.00
https://doi.org/10.1145/3394486.3403281

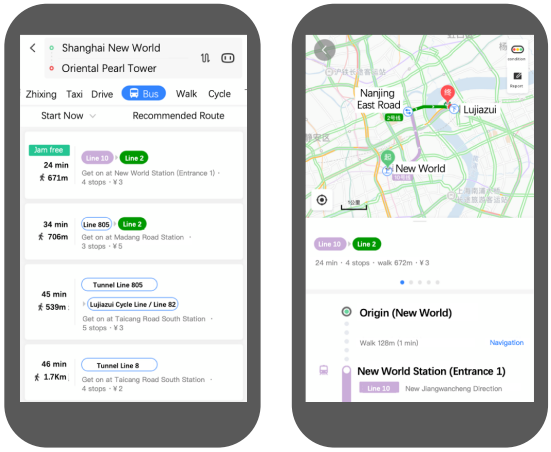

(a) Ranked route list. (b) Details of the first route.

Figure 1: Examples of user interfaces of Polestar**. (a) A ranked list of public transportation routes from Shanghai New World to the Oriental Pearl Tower, two landmarks in Shanghai, China. (b) The details of the first route in (a), which is a metro based transportation route. The first route is fastest and is with least number of transfer.**

1 INTRODUCTION

Public transportation is a form of transit that offers people travel together along designated routes. In recent decades, public transportation has become ubiquitous, and we have witnessed the rapid increase in access to and use of the public transportation system. For example, in 2018, the China government invested more than $74 billion[1] in public transportation infrastructure and the public transportation systems took over 120 billion trips[2]. In fact, public transportation is playing a key role in the daily life of urban residents. Public transport modes such as bus, metro, and light rail can help reduce urban traffic jam, improve urban transportation network efficiency, and ultimately reduce urban commute costs [3, 15].

However, despite the popularity and various advantages of public transportation, it is challenging for users to find the most preferred routes from a variety of routes, because of the complex public transportation networks, new emerging public transportation tools (*e.g.*, vanpooling, on-demand ride-hailing, shared bike, *etc.*), and the dynamic travel context (*e.g.*, transportation station distribution, weather, travel intention, *etc.*). As a result, public transportation routing services such as Baidu Maps and Google Maps become essential tools in people's daily lives.

[1]http://www.xinhuanet.com/english/2019-02/13/c_137819050.htm
[2]http://xxgk.mot.gov.cn/jigou/zhghs/201905/t20190513_3198918.html

While geographic routing is well-studied, the predominant research and applications are mostly about routing with road networks, only a few works focus on public transportation routing. For example, Efentakis *et al.* [10] formulated the public transportation routing problem as a database query and proposed a pure SQL based routing framework. Wang *et al.* [24] and Delling *et al.* [8] modeled public transportation networks as a timetable graph and proposed a labeling based index to speedup shortest path queries. However, all the above approaches mainly focus on city-wide public transportation routing, and only consider single or a few transport modes (bus and metro). More importantly, all the above approaches focus on optimizing static criteria (*e.g.*, earliest arrival, latest departure, shortest travel time), but overlook the user preference under dynamic situational context, which is important for user decision making. For example, metro may be a more preferable choice during morning rush hour or under severe weather condition, whereas the cheapest route may be a better choice when one's trip purpose is not in an emergency.

In fact, building a public transportation routing engine has far beyond searching shortest paths. The major challenge comes from two aspects. First, the rapid expansion of the public transportation network induces highly overlapped transportation lines. The alternative sub-routes and the ultimate line transfer lead to the combinatorial explosion of the route search space. The first challenge is how we can efficiently generate feasible route candidates. Second, the user preference is highly dynamic and depends on many factors such as price, time period, and weather condition. Simply sorting routes based on static criteria such as distance or time fails to deliver a satisfactory user experience. So, the second challenge is how to rank route candidates by characterizing user preference under dynamic travel context.

To tackle above challenges, in this paper, we present Polestar, an intelligent public transportation routing engine. We hope to share our practical experience on how to build an intelligent, efficient, and national-wide public transportation routing service. In early 2019, Polestar has been deployed on Baidu Maps, one of the world's largest navigation apps, servicing over 330 cities in mainland China. Figure 1 shows the user interface of Polestar on Baidu Maps app.

Contributions. To the best of our knowledge, this is the first work introducing a deployed national-wide public transportation routing engine that answers a hundred millions of queries each day. Specifically, we first propose the public transportation graph, PTG, that assembles heterogeneous public transportation lines into a unified structure. PTG elegantly models various travel costs and reduces routing complexity by mapping public transportation lines into a set of physical and virtual graphs. Beside, we design efficient route candidate generation algorithms, coupled with an efficient station binding method. In average, route candidate generation can be done in tens of milliseconds in Polestar. Moreover, we propose a two-pass route candidate ranking pipeline to capture user preference under dynamic travel context. The route candidate ranking pipeline achieves 9.4% relative improvement of user click ratio in the production environment. Finally, we develop a series of optimization techniques to reduce web service latency and discuss several deployment issues. Extensive experiments on urban-scale real-world datasets show that Polestar achieves less than 250ms latency in average and exhibits excellent ranking performance compared with six baselines.

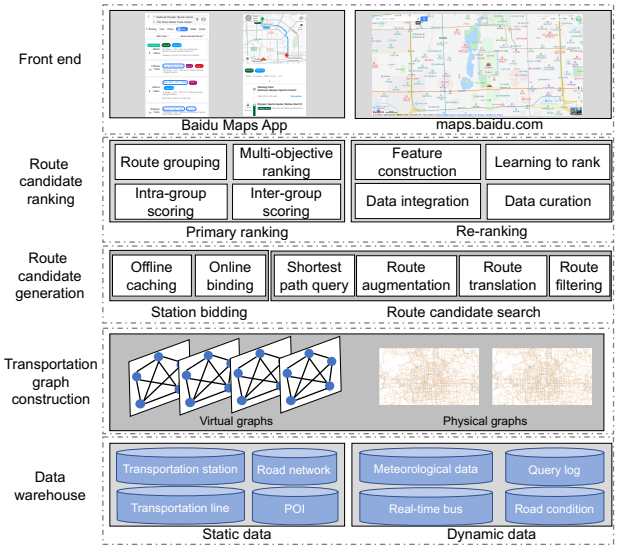

Figure 2: The framework overview of Polestar**.**

2 FRAMEWORK

Figure 2 shows the framework of Polestar, which consists of five components, the *Data warehouse*, the *Public transportation graph construction*, the *Route candidate generation*, the *Route candidate ranking* and the *Front end*. The *Data warehouse* stores a wide range of datasets on a distributed cluster, such as the transportation station data and the transportation line data. Based on transportation line related datasets in the *Data warehouse*, the *Graph construction* module compiles the PTG, which including a set of intra-city graphs. When a routing query is submitted, the *Route candidate generation* module searches a set of feasible route candidates based on the PTG. Concretely, we first bind the origin and the destination to proper stations based on a pre-computed station cache. After that, a bidirectional shortest path search algorithm is applied on a set of virtual graphs simultaneously to generate set of feasible route candidates, which later will be translated to human-readable routes based on the physical graph. Once a set of route candidates is obtained, a two-pass *Route candidate ranking* module is invoked for context-aware ranking. Specifically, the primary ranking first partitions route candidates into several route groups and then select a small subset of diversified route candidates. After that, the re-ranking step constructs a rich set of features and applies a machine learning based model to decide the final rank of each route candidate. Finally, the ranked route list is returned to the *Front end*. There are two interfaces in the *Front end*: the App interface for mobile devices and the webpage interface for PC.

3 DATA DESCRIPTION AND ANALYSIS

This section introduces datasets used in Polestar, with a preliminary data analysis. In this paper, we use two datasets, Shanghai and Guangzhou. Both of them are randomly sampled from 60 consecutive days in early 2019. The statistics of two datasets are summarized in Table 1.

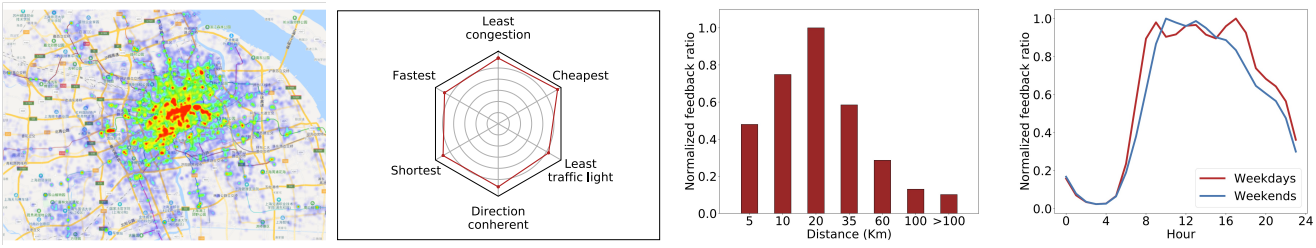

(a) Spatial distribution of destinations (b) Feedback distribution (c) Distance distribution (d) Day distribution

Figure 3: Distributions of the SHANGHAI dataset: (a) the spatial distribution of query destinations; (b) the distribution of routes with user feedbacks; (c)the distribution of travel distances; (d) the distribution of travel time (hour).

Table 1: Statistics of datasets.

Data description		SHANGHAI	GUANGZHOU
Query log data	# of sessions	5,900,463	2,750,316
Geographical data	# of stations	68,687	65,525
	# of lines	3,341	2,839
	# of road segments	406,195	284,168
	# of POIs	1,594,684	982,059
Meteorological data	# of records	23,424	16,104

Geographical data. We use large-scale geographical datasets to build Polestar, including: (1) the transportation station data, (2) the transportation line data, (3) the road network data, and (4) the point of interest (POI) data [31]. All geographical data are collected from (i) professional surveyors employed by Baidu Maps, (ii) the crowdsourcing platform in Baidu. Public transportation stations are fundamental data to build the PTG. Besides, geographical data contains rich semantic information regarding user mobility [28, 32]. For example, regional transportation station density influences the public transportation accessibility of a specific area, and the POI type of destination reflects user travel intention [23].

Query log data. Query log data captures user interactions with Baidu Maps. According to the user interaction loop, the query log data generated during user-App interactions can be further categorized into *query records*, *routes records*, and *feedback records*. Briefly, a query record indicates a route query from a user on Baidu Maps, a routes record contains a list of feasible candidate routes present to the user, and a feedback record represents user's preference of given candidate routes. Different from traditional recommenders [14] collect user clicks as feedback, we extract more reliable feedbacks to distinguish better routes, which include *add route to favorites*, *share route with others*, *screenshot* and *navigation*.

Meteorological data. Meteorological conditions are critical factors for trip planning. For example, a route with less walk distance is preferable in the case of snow, rain, and severe air pollution. Each meteorological data point consists of a location, a timestamp, the weather, the temperature, the wind strength, the wind direction, and the Air Quality Index (AQI). We use the meteorological data from an online meteorology website of the Chinese government.

Data analysis. To further understand the distributions of each dataset, we use the dataset SHANGHAI for illustration. We observe similar data distributions in other cities and time periods. Figure 3(a) shows the distributions of destinations in query records. As can be seen, most destinations fall in the downtown areas in SHANGHAI. Figure 3(b) plots the distribution of user-preferred routes (*i.e.*, route with user feedbacks), the ratio of least congestion, fastest, shortest, direction coherent, least traffic light and cheapest are 58.9%, 55.6%, 57.1%, 56.6%, 52.2% and 61.5%, respectively. Since a route may be the best in multiple aspects (*e.g.*, least congestion and fastest), the overall ratio is greater than 100%. Overall, we observe multiple factors users may concern when planning a trip. Figure 3(c) depicts the spatial distribution of user feedbacks. We observe over 80% trips are within 35Km and trips of the distance around 20Km are most popular, which provides extra information for public transportation routing. Finally, Figure 3(d) shows the temporal distribution of user feedbacks. Overall, we observe the user feedback ratio at daytime is higher than night, and the distribution on workday and weekend are also different. Above observations motivate us to incorporate multi-source urban data to model the dynamic travel context, and build a machine learning based model for intelligent route recommendation.

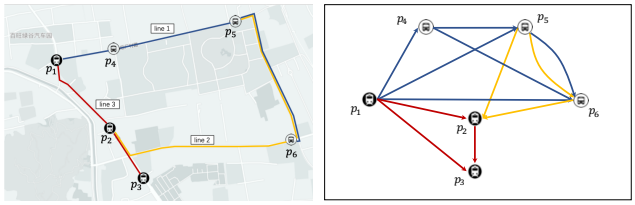

(a) Transportation lines on the map. (b) Physical transportation graph.

Figure 4: Example of transportation graph construction.

4 PUBLIC TRANSPORTATION GRAPH CONSTRUCTION

One major design objective of Polestar is to provide an efficient national-wide public routing service. However, it is computationally expensive to route on a unified public transportation graph [10, 24] that contains millions of transportation lines. In this section, we propose the *public transportation graph* to reduce the route candidate generation complexity on various travel costs. Specifically, the unified graph structure partitions transportation lines into a set of disjoint intra-city publication transportation graphs, the route candidate search space is therefore bounded into a relatively smaller range. Moreover, the public transportation graph decouples each subgraph into one *physical graph* and multiple *virtual graphs*, where each virtual graph corresponds to a different travel cost.

Consider a set of public transport modes $M = \{m_1, m_2, \ldots, m_i\}$. A *physical transportation station* $p_i \in P$ is represented as a geographical coordinate (φ_i, λ_i). Note that p_i can be passed by multiple transportation lines. A *Transportation line* is defined as a tuple

(m_i, l_i), where $m_i \in M$ is a public transport mode, $l_i = p_1 \rightarrow p_2 \rightarrow \cdots \rightarrow p_n$ is an ordered physical transportation station list. In practice, a transportation line may be a bus line, a metro line, a ferry route, etc.

Definition 1. ***(Physical transportation graph)*** *A physical transportation graph is a 5-tuple $G^P = (P, E, O, D, L_E)$, where P is a set of physical transportation stations, E is a set of edges between physical transportation stations, O is a mapping set $P \rightarrow E$ assigning to edge its origin station, D is a mapping set $P \rightarrow E$ assigning to edge its destination station, and L_E is a mapping set marks the transportation line of each edge.*

The physical transportation graph is a directed multi-graph, where each edge is with its own identity. Give two physical transportation stations p_i and p_j, there is an edge from p_i to p_j if and only if there exists a transportation line pass from p_i to p_j without transfer. Note that there may have multiple edges from p_i to p_j if there are multiple transportation lines pass from p_i to p_j. Consider a set of transportation lines shown in Figure 4(a), Figure 4(b) depicts the corresponding physical transportation graph. For example, as line 3 passes p_1, p_2 and p_3, there are three edges (p_1, p_2), (p_1, p_3) and (p_2, p_3) labeled as line 3. Besides, there are two transportation lines that pass from p_5 to p_6, from which we derive two edges between the corresponding nodes.

The advantages of the physical transportation graph are twofold. First, it fits heterogeneous transportation lines into a unified graph representation, which eases subsequent route candidate generation. Second, directly connecting transportation stations in the same transportation line significantly reduces the search depth in route generation, therefore increasing the number of feasible route candidates in fixed search depth.

Similar to the physical transportation station, we define *virtual transportation station $v_i \in V$* based on the physical transportation station, each of which corresponds to an individual transportation line. In other words, a physical transportation station is mapped to multiple virtual transportation stations, and each virtual transportation station corresponds to a different transportation line.

Definition 2. ***(Virtual transportation graph)*** *A virtual transportation graph is defined as a 4-tuple $G^V = (V, E, S_{PV}, c_E)$, where V is a set of virtual transportation stations, E is a set of edges between virtual transportation stations, S_{VP} is a table $V \rightarrow P$ which maps virtual transportation stations to physical transportation stations, and c_E is a mapping set describes the weight of each edge.*

The relation between virtual transportation station and physical transportation is many-to-one. For example, given the physical transportation graph shown in Figure 4(b), virtual station $v_1^{p_5}$ and $v_2^{p_5}$ are mapped to physical transportation station p_5. Two edges between p_5 and p_6 are mapped to two disjoint virtual edges $(v_1^{p_5}, v_1^{p_6})$ and $(v_2^{p_5}, v_2^{p_6})$, associated with different travel cost. In Polestar, a virtual transportation graph is stored in two parts, the station mapping table, and the virtual graph table.

Currently, each physical transportation graph corresponds to three virtual transportation graphs, *i.e.*, the distance graph, the travel time graph, and the walk distance graph. All three virtual graphs are isomorphism, except that the weight of each edge is computed from different cost function. The weight of each edge is estimated from query log data and historical road conditions. Note that other types of virtual graphs can be extended on demand.

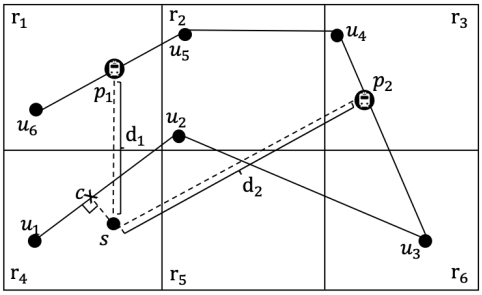

Figure 5: Example of station binding. s is the current location, u_1-u_6 are road intersections, p_1-p_2 are physical transportation stations, r_1-r_6 are partitioned grids, c is projected point from s to (v_1, v_2).

Based on the physical graph and virtual graphs for public transportation networks in each city, we construct the *public transportation graph.*

Definition 3. ***(Public transportation graph (PTG))*** *A PTG is defined as a set of physical transportation graphs and virtual transportation graphs $G^H = \{G_1^P, G_2^P, \ldots, G_1^V, G_2^V, \ldots\}$. PTG partitions the public transportation graph into a set of disjoint public transportation graphs. Each sub-graph corresponds to an intra-city public transportation network.*

PTG partitions large-scale graphs into a set of subgraphs and therefore reduces the candidate route generation complexity.

5 ROUTE CANDIDATE GENERATION

In this section, we describe the detailed process of route generation, including station binding and route candidate search.

5.1 Station binding

In general, the origin and the destination of a query are arbitrary geographical locations. A primary step for route candidate generation is binding the origin (resp. destination) location to physical transportation stations the user can get on (resp. get off). A straightforward approach is computing the Euclidean distance between the origin (resp. destination) location with each surrounding physical station and select top-k nearest stations as getting on (resp. getting off) stations. However, as the distance between the location and each station is constrained by the pedestrian road network, the actual road network distance may be much longer than the point-to-point Euclidean distance, which may lead to a sub-optimal binding result. For example, in Figure 5, the Euclidean distance from location s to p_1 is less than from s to p_2, however, the road network distance from location s to p_1 is greater than from s to p_2. Another option would be to map the location to a road segment and then compute the road network distance on the fly. However, this approach leads to great online computation overhead and induce efficiency degradation. In Polestar, we employ a caching method to bind geographical locations to stations more accurate and efficient.

The proposed station binding method builds an online-offline framework as follow. Given a location s, a road network $G^R = (V, E)$, and stations $p_i \in P$, we first build an offline nearest station cache. Specifically, we partition the city into a set of disjoint grid $r_k \in R$, and place each road intersection $u_i \in V$ on this grid. For each road intersection u_i, we apply Dijkstra's algorithm to select a set of stations such that $d(u_i, p_j) < \lambda$, where $d(\cdot)$ is the road network distance and λ is a maximum distance threshold. Note that we project all stations to the nearest road segment. We then group the distance information of each station by region and stored them in the cache. In the online binding process, we first map the location s to the nearest POI. Each POI is projected to a reachable road segment associated with a walking distance. Take Figure 5 again for example, s is projected to (u_1, u_2) at c, the overall distance from the location s to a station p_1 can be derived as

$$d(s, p_1) = d(s, c) + d(c, u_2) + d(u_2, p_1), \tag{1}$$

where $d(s, c)$ is the walk distance from location s to road segment, $d(c, u_2)$ is the road network distance from the projected point c to road intersection u_2, and $d(u_2, p_1)$ is the road network distance pre-stored in cache. As $d(s, p_1) > d(s, p_2)$, p_2 is selected as the best match for the station.

5.2 Route candidate search

Given origin and destination stations, we model the route candidate search as a vertex-to-vertex shortest path search problem. The intra-city routing generates route candidates in three steps. First, a bidirectional Dijkstra's algorithm [19] is applied to each virtual graph to generate feasible route candidates. The search procedure stops when a criterion is satisfied, *e.g.*, maximum search time or the maximum number of route candidates. Second, route candidates are mapped to physical transportation stations and physical transportation lines via the route translation module. Detailed route information such as price, ETA, route shape is attached to each route candidate. Third, a route filter and route augmentation module are invoked to augment route candidate diversity and filter out less competitive route candidates (*e.g.*, routes containing cycles). For route augmentation, a greedy algorithm is applied to replace each route segment. Recall the the physical transportation graph is a multi-graph, route augmentation replaces one edge with same origin and destination station in each step. The detailed procedure of route candidate search is shown in Algorithm 1.

Take Figure 4 as a running example. Assume p_1 as the origin station and p_6 as the destination station, bidirectional Dijkstra's algorithm is first performed on three virtual graphs in parallel. Assume three route candidates on virtual graph $(v_1^{p_1}, v_1^{p_6})$, $(v_1^{p_1}, v_2^{p_5}, v_2^{p_6})$ and $(v_1^{p_1}, v_2^{p_2}, v_2^{p_6})$ are found, three route candidates are translated to (p_1, p_6) in Line 1, (p_1, p_5, p_6) in Line 1 then Line 2, and (p_1, p_2, p_6) in Line 3 then Line 2, via the physical graph. After that, each route segment is replaced by alternative transportation lines to augment route candidate. For example, in the route (p_1, p_5, p_6), the segment (p_5, p_6) in Line 2 can be replaced to Line 1 and will be filtered out later since the new route is identical to (p_1, p_6) in Line 1. As a result, three feasible route candidates are returned.

Algorithm 1: Route candidate search

Input: Physical graph G^p, virtual graphs $G_1^v, G_2^v, \ldots,$ origin station o, destination station d, maximum search time t, maximum route candidate set size k.
Output: C: a set of feasible route candidates.

```
Set C ← ∅;
while |OpenSet| ≤ k or running_time ≤ t do
    for each virtual graph G_i^v do
        virtual_routes ← BidirectionalDijkstra(G_i^v, o, d);
        physical_routes ← Translation(G^p, virtual_routes);
        candidate_routes ← Augmentation(G^p, physical_routes);
        for each c_i ∈ candidate_routes do
            C ← C ∪ c_i;
return C;
Function BidirectionalDijkstra (G^v, o, d):
    while forward search and reverse search meet on vertex x do
        forward search from o on the original graph with a label d_f;
        reverse search from d on the reversed graph with a label d_r;
    return route meet on x of cost d_f + d_r;
Function Augmentation (G^p, physical_routes):
    new_routes ← ∅ for physical_route ∈ physical_routes do
        for route_segment ∈ physical_route do
            new_route ← replace route_segment to another edge in G^p with same origin station and destination station;
            new_routes ← new_routes ∪ {new_route}
    return new_routes;
```

6 ROUTE CANDIDATE RANKING

In this section, we describe details of the *route candidate ranking* module, including the primary ranking and the re-ranking. The primary ranking derives a diversified route candidate subset whereas the re-ranking orders route based on users' preference under dynamic travel context.

6.1 Primary ranking

In general, the route candidate generation produces a route candidate set contains over 50 route candidates, which is time-consuming to apply a full-fledged machine learning based ranking model directly. Therefore, we first employ a light-weight primary ranking to reduce the size of the route candidate set further. Concretely, primary ranking reduces the size of the route candidate set in three steps. First, filter out inferior route candidates, such as similar routes, detour routes, and routes with bad transfer combinations (*e.g.*, metro-bus-metro). Second, group route candidates based on transport modes, such as bus, metro, mixed transport modes and

so on. The grouping step guarantees the diversity of the final route candidate set. Third, sort routes in each group according to a cost function. The cost function considers multiple factors such as travel time, distance, and the walk distance. The winning route candidates in each group will be passed for re-ranking. Note that all preserved route candidates will be visualized in front-end, re-ranking will further decide the order of each route candidate. In Polestar, the primary ranking reduces the route candidate set size to 5-7. The primary ranking step can be done in 100ms.

6.2 Re-ranking

After a smaller route candidate set is obtained, we apply a more expensive machine learning based re-ranking model. In this phase, more complex information such as real-time bus, available ticket, and the ticket price are incorporated. We first describe situational features we construct for re-ranking.

6.2.1 Feature construction. Feature engineering is a critical step to build an expressive ranking model. Proper feature engineering process can improve the model performance and speed up the convergence of optimization [29]. Based on explorative data analysis in Section 3, we construct five categories of situational features: route features, spatial features, temporal features, meteorological features, and augmented features.

Route features. For each route, we extract *ETA*, *Estimated waiting time*, *Price*, *Ticket availability*, *Road network distance*, *Road congestion index*, *Start walk distance*, *End walk distance*, *On transport distance* and *Number of transfer* from plan records. The *Road network distance* is the real travel distance. The *Road congestion index* is the congestion score of each route. For transportation not on road network (*e.g.*, metro), the index is set to zero. The *Start walk distance* (resp. *End walk distance*) is the walk distance in the beginning (resp. in the end). The *Estimated waiting time* is calculated based on real-time bus information and bus time table.

Spatial features. User's preference at different locations may vary. We first extract the *city* and the *district* the origin and destination belongs to. Based on the POI data, we extract *Primary POI category* and *Secondary POI category*. Similar to station binding, we partition the city into a set of grid. For each origin and destination, we further construct statistical features for corresponding grid. Specifically, we construct the *regional POI distribution* vector, in which each dimension indicate the POI count of each POI category. We further compute *regional transportation station distribution*, in which each dimension represents the count of transport stations (*e.g.*, bus stations, metro stations, *etc.*). We also compute *road network density* and *station density* for each grid. Note that the transportation station data used for re-ranking is same as used for PTG compilation.

Temporal features. The user preference at a different time may also differ. For example, the metro may be a better choice at morning rush hour, whereas the night bus is a possible choice at midnight. We construct *Hour*, *Minute*, *Day of week*, *Day of month*, *Holiday*, *Route in service* as temporal features.

Meteorological features. We construct meteorological features from the meteorological dataset. We extract *Weather*, *Temperature*, *Wind speed*, *Wind direction* and *Air Quality Index* (AQI) as the meteorology features. Specifically, *Weather* and *Wind direction* are categorical features whereas *Temperature*, *AQI*, *Wind speed* and *Humidity* are numerical features. The weather is categorized as Sunny, Rainy, Overcast, Cloudy, Foggy and Snow. We discretize wind direction to 16 categories. The AQI is an integer value. There are 13 wind strength levels from 0 to 12. The AQI is an integer that represents the air pollution level.

Feature augmentation. We further augment features from two aspects. First, we compute statistical features to characterize the distribution of each feature. For route list, we compute *Min*, *Max* and *Average* of each route, and compute the difference between basic features and statistical features. For example, for distance we compute *Max road network distance*, *Min road network distance*, and *Average road network distance* over all routes in the route list. We compute $ETA - MinETA$ to measure the relative travel time advantage of a route. Second, we combine features from different domains to build combinational features. For example, we combine route features and temporal features to capture the route statistics at different time period (*i.e.*, hour, day of the week). We combine route and spatial features to capture the dependency between the POI category and transport mode preference. Combinational features further capture correlations between each feature category.

6.2.2 The model. Given a query q_i, a list of route candidates $\mathbf{X}^i = \{\mathbf{x}_1^i, \mathbf{x}_2^i, \dots\}$, the re-ranking model aims to decide the order of each route candidate. Specifically, each $\mathbf{x}_j^i$ is represented as a m dimensional feature vector, *e.g.*, ETA, destination POI type, and weather. We propose a pair-wise learning to rank model based on GBDT (Gradient Boosting Decision Tree) [11]. GBDT has proven performs well on tasks with sparse and high-dimensional features. In the learning procedure, the GBDT generates a set of tree classifiers $\mathcal{G} = \{g_1(\cdot), g_2(\cdot), \dots, g_k(\cdot)\}$ sequentially. The rationale behind GBDT is that the model is able to construct a robust classifier by using an ensemble of weak classifiers $g(\cdot)$ to generate the final prediction result

$$\hat{y} = f(\mathbf{x}^i) = \sum_{j=1}^{k} g_j(\mathbf{x}^i), g_j \in \mathcal{F}, \tag{2}$$

where $\hat{y}$ is the estimated result of instance $\mathbf{x}^i$, $g_j(\cdot)$ is a tree classifier learned in step j.

Rather than training each route candidate individually, we build a more informative training set that includes the relative preference relationship. Specifically, given q_i and $\mathbf{X}^i$, we construct training instances as

$$\mathcal{S} = \{(\mathbf{x}_1^i, \mathbf{x}_2^i) | \mathbf{x}_1^i \succ \mathbf{x}_2^i, i = 1, \dots, |\mathbf{X}^i|\}, \tag{3}$$

where $\succ$ indicate $\mathbf{x}_1^i$ is a more preferable choice than $\mathbf{x}_2^i$ for q_i. In fact, $\mathcal{S}$ is a partially ordered set. The partial order relationship is derived by the order of user feedback records. For example, if a user add $\mathbf{x}_1^i$ to favorite before $\mathbf{x}_2^i$ in same query, we have $\mathbf{x}_1^i \succ \mathbf{x}_2^i$. With the training set, we define the pair-wise ranking loss function as

$$L(q_i, \mathcal{S}) = \frac{1}{2} \sum_{j=1}^{N} (max\{0, \tau - (f(\mathbf{x}_1^i) - f(\mathbf{x}_2^i))\})^2 - \lambda_1 \tau^2 + \frac{\lambda_2}{2} \|\mathbf{X}^i\|_2, \tag{4}$$

where $f(\cdot)$ is the expected ranking function need to learn. To avoid a trivial optimal $f(\cdot)$ to be obtained, *i.e.*, a constant function, we further add a constant gap $\tau \in (0, 1]$ to the loss function. λ_1 and λ_2

are hyper-parameters for the constant gap and the $L2$ regularization, respectively. We introduce $L2$ regularizer into the loss function to alleviate overfitting in model training.

Given the above loss function, a functional gradient descent [30] is then applied to optimize the ranking function. In step k, a gradient boosting tree $g_k(\cdot)$ is generated, the ranking function is updated as

$$f_k(\mathbf{x}^i) = \frac{k f_{k-1}(\mathbf{x}^i) - \beta g_k(\mathbf{x}^i)}{k+1}, \tag{5}$$

where β is the learning rate.

7 DEPLOYMENT

In this section, we discuss several important implementation and deployment issues, in both the offline processing phase and the online processing phase.

7.1 Offline processing

The offline processing handles four major tasks, the *data management*, the *transportation graph compilation*, the *station cache update*, and the *re-ranking model training*.

Data management.The *Data warehouse* stores all datasets on a Hadoop cluster. The datasets can be categorized into static datasets and dynamic datasets. Static datasets include transportation station data, transportation line data, road networks, and POI data, whereas dynamic datasets include query log data, real-time bus data, and traffic condition data. Static datasets are updated periodically (from day to months), and dynamic datasets are updated in real-time.

Transportation graph compilation. Real-world transportation systems are highly dynamic. Each day, new transportation lines open and existing transportation lines are cancelled or adjusted. We propose a graph compilation pipeline to automatic the PTG updating process. In each day, the up-to-date transportation station data, transportation line data, road network data, and a snapshot of traffic condition data are loaded into the data warehouse. The mapping between transportation stations and transportation lines is recompiled to update physical graphs; the mapping between transportation lines and road network is recompiled to update the edge weight of virtual graphs.

Station cache update. Similar to the transportation graph compilation pipeline, the station cache used for station binding is also updated every day to accurately measure the cost to each station. The station cache is stored as a hash table in a Redis database.

Re-ranking model training. The re-ranking model relies on multiple large-scale heterogeneous data sets. We employ a distributed platform, Bigflow (http://bigflow.baidu.com), for the data preprocessing. Specifically, we first integrate each data set into a large fact table by using the *JOIN* operator, then transform the fact table to a feature table, as described in Section 6.2.1. All numerical features are scaled to $[0, 1]$ and all categorical features are processed as one-hot encoded vectors. Once the input feature is ready, we employ XGBoost [4], a high performance distributed gradient boosting library for model training. We use 5-fold cross-validation, and the re-ranking model is updated on a daily basis. The model takes the two most recent months of data as input to exclude seasonal changes. We use a server with 64 Intel Xeon E5-2620v4 CPU, 120GB memory, and 2TB disk for model training.

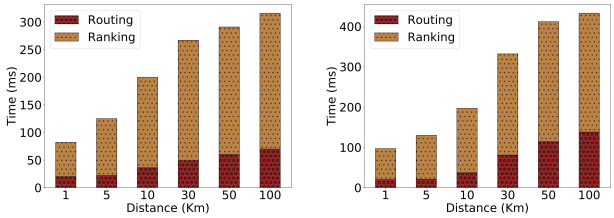

(a) Routing on Shanghai (b) Routing on Guangzhou

Figure 6: Running time v.s. distance.

7.2 Online processing

At running time, the response time (*a.k.a.* service latency) is crucial to user experience. We adopt BRPC (https://github.com/brpc/brpc), an open-sourced scalable web service framework for online service. In online processing, six components are involved. First, when a query is submitted, the origin and destination are binded to transportation stations. Second, the routing executor generates a set of feasible route candidates. Third, the primary ranking is then applied to select a small set of route candidates. Fourth, the feature vector for re-ranking is retrieved from the data or collected from other online services. Fifth, the final order of each route is decided by the re-ranking model. Finally, each route is returned to the frontend associated with auxiliary data such as road congestion and real-time bus information. The PTG, the station cache, and the re-ranking model are duplicated in multiple data centers through BRPC. These data centers are distributed in different provinces in China to reduce the latency from different geographical locations and balance the workload.

8 EXPERIMENTS

In this section, we conduct extensive experiments to evaluate: (1) the efficiency of Polestar, including the running time of route candidate generation and route candidate ranking, (2) the effectiveness of Polestar, including the overall ranking performance and the feature importance analysis, and (3) the online assessment.

8.1 Efficiency

We first evaluate the overall running time of Polestar. Specifically, we exam the performance of Polestar for processing queries of different distances, including both end-to-end and component-wise running time. For each distance interval, we randomly extract 1, 000 queries from the log and calculate the averaged running time.

Figure 6(a) and Figure 6(b) report the running time of queries on Shanghai and Guangzhou. We observe that Polestar achieves promising running time for queries of different distances. For queries shorter than 10 Km, the overall running time is less than 200 ms. When query distance increases to 100 km, the running increases to 300 ms, indicating Polestar achieves sub-linear scalability in terms of query distance. In Figure 6(a) and Figure 6(b), we break the running time into routing and ranking phases for further comparison. It can be seen that the routing phase takes less than 50ms for all queries, whereas the running time of ranking varies from 50ms to 200ms. This indicates that the ranking phase can be further optimized to reduce the overall latency. Overall, Polestar achieves promising efficiency performance.

Table 2: Overall ranking performance.

	Model	NDCG@1	NDCG@3	NDCG@5
Shanghai	Shortest	0.428	0.599	0.803
	Fastest	0.306	0.513	0.761
	Least transfer	0.778	0.853	0.926
	LR	0.878	0.902	0.955
	GBDT	0.921	0.922	0.966
	DNN	0.9261	0.9189	0.9666
	Polestar	**0.937**	**0.959**	**0.979**
Guangzhou	Shortest	0.472	0.632	0.818
	Fastest	0.334	0.540	0.771
	Least transfer	0.832	0.889	0.944
	LR	0.887	0.91	0.958
	GBDT	0.916	0.92	0.965
	DNN	0.9245	0.9205	0.9669
	Polestar	**0.934**	**0.954**	**0.977**

8.2 Effectiveness

Then we evaluate the overall ranking performance of Polestar and analyze the usefulness of our features.

Metric. We adopt Normalized Discounted Cumulative Gain (NDCG) [25, 27], a widely used metric in search engines and recommender systems, to evaluate the ranking performance. In this paper, we compare NDCG@1, NDCG@3 and NDCG@5.

Baselines. We compare Polestar with three statistical baselines and three machine learning based baselines. **Shortest** rank route candidates according to the overall route distance. **Fastest** rank route candidates according to the overall travel time. **Least transfer** rank route candidates according to the number of transfer of each route. **LR** rank route candidates via the well-known logistic regression model. The input feature is same as Polestar described in Section 6. **GBDT** uses the same learning model in Polestar, the only difference is GBDT employs a point-wise cross-entropy loss function [20]. **DNN** constructs deep neural network contains two fully connected hidden layers as in [2], applies Relu as the activation function, and employ Adam for optimization.

8.2.1 Overall ranking result. Table 2 depicts the overall ranking performance of Polestar and six baselines with respect to NDCG@k. As can be seen, Polestar significantly outperforms six baselines on both Shanghai and Guangzhou using all three NDCG metrics. Specifically, Polestar achieves 0.93+ NDCG@1 score on both datasets, indicating that most routes with user feedbacks are successfully ranked at top-1 in our engine. Besides, we observe that all machine learning based models achieve better ranking performance than statistical based methods, which further proves that our tailored feature construction procedure successfully captures dynamic context factors in user queries. Moreover, the performance of Polestar is (1.6%, 3.7%, 1.3%) and (1.8%, 3.4%, 1.2%) higher than GBDT on two datasets on (NDCG@1, NDCG@3, NDCG@5), demonstrating the power of our pair-wise ranking function. Finally, we observe Polestar achieves slightly better results than DNN, further illustrate the effectiveness of tree based models on capturing non-linear dependencies. Besides, the computational cost of Polestar is significantly lower than deep neural network, which is an important advantage of Polestar as an online service.

8.2.2 Feature importance analysis. To evaluate the effectiveness of our features, Table 3 reports the top-10 most important features in Polestar. We rank features by information gain [18]. Higher information gain means higher frequency the feature used to split nodes in each boosting trees. As we can see, all features are route related features except the 6th feature. The 6th feature is a context feature describes the query time. Travel time factors are top-2 features, which validates our intuition that time is the most important factors when the user plans a trip. Moreover, the 2nd and 4th features are augmented features, illustrate the effectiveness of our feature augmentation procedure. Finally, we observe that the relative gain of all top-10 features are higher than 0.4, indicating no feature dominates the re-ranking process.

Table 3: Top-10 features ranked by information gain.

Rank	Feature name	Relative gain
1	ETA	1
2	ETA - Min ETA	0.899
3	Walk distance	0.785
4	Walk distance - Min walk distance	0.654
5	On transport distance	0.612
6	Hour	0.609
7	Number of transfer	0.563
8	On transport distance	0.489
9	End walk distance	0.446
10	Start walk distance	0.423

8.3 Online assessment

Table 4: Online user interview result.

City	G	S	B	Improvement
Shanghai	123	62	15	24%
Guangzhou	52	40	8	32%

In the production environment, we observe Polestar achieves 9.4% relative improvement of user click ratio, where the user click ratio is defined as the number of clicks over the number of Polestar routed queries. Besides, Polestar reduces the size of the transportation graph to 3.3 GB, which is only 15.7% as large as the previous one. Moreover, Polestar improves the single server QPS (query per second) from 30 to 40, achieving a 33.3% improvement.

To evaluate the quality of new ranking results, we conduct user interview one week after Polestar fully deployed. Specifically, we published survey questionnaires in Baidu Maps. In the questionnaire, we set three level ranking category, G, S, B, where G stands for better than the previous ranking result, S stands for same as the previous ranking result, and B stands for worse than the previous ranking result. The user interview result in Shanghai and Guangzhou is reported in Table 4. The improvement of the new ranking result is defined as $\frac{\#\ of\ G - \#\ of\ B}{\#\ of\ feedbacks}$. Overall, Polestar achieves 24% and 32% gain in Shanghai and Guangzhou, respectively.

9 RELATED WORK

Transportation routing can be partitioned into *model-free* routing and *model-based* routing.

Model-free routing aims to build efficient algorithms to answer specific queries, *e.g.*, earliest arrival, latest departure, and shortest duration [24]. For public transportation, the network is usually formalized as a timetable graph [10]. On the one hand, efficient index structures such as hub labeling [1] and contraction hierarchy [13] are proposed to speed up such shortest path search. On the

other hand, Funke *et al.* [12] and Sacharidis [21] study personalized shortest path routing that supports various optimization criteria. Delling *et al.* [7, 9] study the routing problem with multiple transport mode choices. Efficiency and reachability are major concerns of above model-free routing algorithms in city-wide, whereas the user preference and the dynamic travel context are overlooked.

Model-based routing employs learning or mining models to improve routing performance. For example, MPR [5] discovers sequential patterns from the user trip history and proposes efficient indices to speed up the retrieval of such patterns. T-drive [26] improves route quality based on the taxi driver's intelligence and Dai [6] recommend routes from historical trajectories rather than ad-hoc shortest path search. Moreover, Wang *et al.* [22] incorporates neural network into A^* algorithm for personalized route recommendation. Hydra [17] introduces a data-driven approach that incorporates a network embedding model [16] for multi-modal route recommendation. All of the above approaches focus on finding better driving or traveling routes in a single city and are not designated for public transportation routing.

10 CONCLUSION

In this paper, we presented Polestar, an intelligent, efficient and national wide public transportation engine. We first proposed PTG, a unified graph structure to integrate heterogeneous public transportation lines. Based on PTG, a station binding method and bidirectional Dijkstra algorithm are introduced for efficient route candidate generation. A two-pass ranking framework is then proposed for route candidate selection and ranking. The re-ranking model constructs a rich set of situational features and adopts a learning to rank model to capture user preference under dynamic travel context. Polestar has been deployed and tested at scale on Baidu Maps and answers a hundred millions of queries each day. We believe the proposed framework is not limited to public transportation routing, but also can be referenced for developing other large-scale transport routing engines. We share our practical experience on how to build such a production level routing engine and hope to provide useful insights to communities in both academia and industry.

REFERENCES

[1] Ittai Abraham, Daniel Delling, Andrew V Goldberg, and Renato F Werneck. 2012. Hierarchical hub labelings for shortest paths. In *European Symposium on Algorithms*. 24–35.

[2] Neha Arora, James Cook, Ravi Kumar, Ivan Kuznetsov, Yechen Li, Huai-Jen Liang, Andrew Miller, Andrew Tomkins, Iveel Tsogsuren, and Yi Wang. 2019. Hard to Park?: Estimating Parking Difficulty at Scale. In *Proceedings of the 25th ACM SIGKDD International Conference on Knowledge Discovery and Data Mining*. 2296–2304.

[3] Gabriela Beirão and JA Sarsfield Cabral. 2007. Understanding attitudes towards public transport and private car: A qualitative study. *Transport policy* 14, 6 (2007), 478–489.

[4] Tianqi Chen and Carlos Guestrin. 2016. Xgboost: A scalable tree boosting system. In *Proceedings of the 22nd ACM SIGKDD International Conference on Knowledge Discovery and Data Mining*. 785–794.

[5] Zaiben Chen, Heng Tao Shen, and Xiaofang Zhou. 2011. Discovering Popular Routes from Trajectories. In *Proceedings of the 27th International Conference on Data Engineering*. 900–911.

[6] Jian Dai, Bin Yang, Chenjuan Guo, and Zhiming Ding. 2015. Personalized route recommendation using big trajectory data. In *Proceedings of the 31st International Conference on Data Engineering*. 543–554.

[7] Daniel Delling, Julian Dibbelt, Thomas Pajor, Dorothea Wagner, and Renato F Werneck. 2012. *Computing and evaluating multimodal journeys.* KIT, Fakultät für Informatik.

[8] Daniel Delling, Julian Dibbelt, Thomas Pajor, and Renato F Werneck. 2015. Public transit labeling. In *International Symposium on Experimental Algorithms*. 273–285.

[9] Julian Dibbelt et al. 2016. Engineering Algorithms for Route Planning in Multimodal Transportation Networks. *Transportation* (2016).

[10] Alexandros Efentakis. 2016. Scalable Public Transportation Queries on the Database. In *EDBT*. 527–538.

[11] Jerome H Friedman. 2001. Greedy function approximation: a gradient boosting machine. *Annals of statistics* (2001), 1189–1232.

[12] Stefan Funke and Sabine Storandt. 2015. Personalized route planning in road networks. In *Proceedings of the 23rd SIGSPATIAL International Conference on Advances in Geographic Information Systems*. 45:1–45:10.

[13] Robert Geisberger, Peter Sanders, Dominik Schultes, and Daniel Delling. 2008. Contraction hierarchies: Faster and simpler hierarchical routing in road networks. In *International Workshop on Experimental and Efficient Algorithms*. 319–333.

[14] Thore Graepel, Joaquin Quinonero Candela, Thomas Borchert, and Ralf Herbrich. 2010. Web-scale bayesian click-through rate prediction for sponsored search advertising in microsoft's bing search engine. Omnipress.

[15] Todd Litman. 2015. *Evaluating public transit benefits and costs.* Victoria Transport Policy Institute Victoria, BC, Canada.

[16] Hao Liu, Ting Li, Renjun Hu, Yanjie Fu, Jingjing Gu, and Hui Xiong. 2019. Joint Representation Learning for Multi-Modal Transportation Recommendation. In *Proceedings of the Thirty-Third AAAI Conference on Artificial Intelligence*. 1036–1043.

[17] Hao Liu, Yongxin Tong, Panpan Zhang, Xinjiang Lu, Jianguo Duan, and Hui Xiong. 2019. Hydra: A Personalized and Context-Aware Multi-Modal Transportation Recommendation System. In *Proceedings of the 25th ACM SIGKDD International Conference on Knowledge Discovery and Data Mining*. 2314–2324.

[18] Gilles Louppe, Louis Wehenkel, Antonio Sutera, and Pierre Geurts. 2013. Understanding variable importances in forests of randomized trees. In *Advances in neural information processing systems*. 431–439.

[19] Rolf H Möhring, Heiko Schilling, Birk Schütz, Dorothea Wagner, and Thomas Willhalm. 2007. Partitioning graphs to speedup Dijkstra's algorithm. *Journal of Experimental Algorithmics (JEA)* 11 (2007), 2–8.

[20] Kevin P Murphy. 2012. *Machine learning: a probabilistic perspective.* MIT press.

[21] Dimitris Sacharidis, Panagiotis Bouros, and Theodoros Chondrogiannis. 2017. Finding The Most Preferred Path. In *Proceedings of the 25th ACM SIGSPATIAL International Conference on Advances in Geographic Information Systems*. 5:1–5:10.

[22] Jingyuan Wang, Ning Wu, Wayne Xin Zhao, Fanzhang Peng, and Xin Lin. 2019. Empowering A* Search Algorithms with Neural Networks for Personalized Route Recommendation. In *Proceedings of the 25th ACM SIGKDD International Conference on Knowledge Discovery and Data Mining*. ACM, 539–547.

[23] Pengfei Wang, Yanjie Fu, Guannan Liu, Wenqing Hu, and Charu Aggarwal. 2017. Human mobility synchronization and trip purpose detection with mixture of hawkes processes. In *Proceedings of the 23rd ACM SIGKDD International Conference on Knowledge Discovery and Data Mining*. 495–503.

[24] Sibo Wang, Wenqing Lin, Yi Yang, Xiaokui Xiao, and Shuigeng Zhou. 2015. Efficient route planning on public transportation networks: A labelling approach. In *Proceedings of the 2015 ACM SIGMOD International Conference on Management of Data*. 967–982.

[25] Yining Wang, Liwei Wang, Yuanzhi Li, and Di He. 2013. A theoretical analysis of NDCG ranking measures. In *COLT*.

[26] Jing Yuan, Yu Zheng, Chengyang Zhang, Wenlei Xie, Xing Xie, Guangzhong Sun, and Yan Huang. 2010. T-drive: driving directions based on taxi trajectories. In *Proceedings of the 18th SIGSPATIAL International conference on advances in geographic information systems*. 99–108.

[27] Zixuan Yuan, Hao Liu, Yanchi Liu, Denghui Zhang, Fei Yi, Nengjun Zhu, and Hui Xiong. 2020. Spatio-Temporal Dual Graph Attention Network for query-POI Matching. In *Proceedings of the 43nd International ACM SIGIR Conference on Research and Development in Information Retrieval, SIGIR 2020, Xi'an, China, July 25-30, 2020*.

[28] Weijia Zhang, Hao Liu, Yanchi Liu, Jingbo Zhou, and Hui Xiong. 2020. Semi-Supervised Hierarchical Recurrent Graph Neural Network for City-Wide Parking Availability Prediction. In *Proceedings of the Thirty-Fourth AAAI Conference on Artificial Intelligence*.

[29] Alice Zheng and Amanda Casari. 2018. *Feature Engineering for Machine Learning: Principles and Techniques for Data Scientists.* O'Reilly Media, Inc.

[30] Zhaohui Zheng, Keke Chen, Gordon Sun, and Hongyuan Zha. 2007. A regression framework for learning ranking functions using relative relevance judgments. In *Proceedings of the 30th annual international ACM SIGIR conference on Research and development in information retrieval*. 287–294.

[31] Jingbo Zhou, Shan Gou, Renjun Hu, Dongxiang Zhang, Jin Xu, Airong Jiang, Ying Li, and Hui Xiong. 2019. A Collaborative Learning Framework to Tag Refinement for Points of Interest. In *Proceedings of the 25th ACM SIGKDD International Conference on Knowledge Discovery & Data Mining*. 1752–1761.

[32] Jingbo Zhou, Anthony KH Tung, Wei Wu, and Wee Siong Ng. 2013. A "semi-lazy" approach to probabilistic path prediction in dynamic environments. In *Proceedings of the 19th ACM SIGKDD international conference on Knowledge discovery and data mining*. 748–756.